

# Complete mitochondrial genome sequence of a Middle Pleistocene cave bear reconstructed from ultrashort DNA fragments

Jesse Dabney<sup>a,1</sup>, Michael Knapp<sup>b,c</sup>, Isabelle Glocke<sup>a</sup>, Marie-Theres Gansauge<sup>a</sup>, Antje Weihmann<sup>a</sup>, Birgit Nickel<sup>a</sup>, Cristina Valdiosera<sup>d,e</sup>, Nuria García<sup>d,f</sup>, Svante Pääbo<sup>a,1</sup>, Juan-Luis Arsuaga<sup>d,f</sup>, and Matthias Meyer<sup>a,1</sup>

<sup>a</sup>Department of Evolutionary Genetics, Max Planck Institute for Evolutionary Anthropology, 04103 Leipzig, Germany; <sup>b</sup>Molecular Ecology and Fisheries Genetics Laboratory, School of Biological Sciences, Bangor University, Bangor, Gwynedd LL57 2UW, United Kingdom; <sup>c</sup>Department of Anatomy, University of Otago, Dunedin 9016, New Zealand; <sup>d</sup>Centro de Investigación Sobre la Evolución y Comportamiento Humanos, Universidad Complutense de Madrid–Instituto de Salud Carlos III, 28029 Madrid, Spain; <sup>e</sup>Department of Archaeology, Environment, and Community Planning, Faculty of Humanities and Social Sciences, La Trobe University, Melbourne, VIC 3086, Australia; and <sup>f</sup>Departamento de Paleontología, Facultad de Ciencias Geológicas, Universidad Complutense de Madrid, 28040 Madrid, Spain

Contributed by Svante Pääbo, August 6, 2013 (sent for review July 11, 2013)

Although an inverse relationship is expected in ancient DNA samples between the number of surviving DNA fragments and their length, ancient DNA sequencing libraries are strikingly deficient in molecules shorter than 40 bp. We find that a loss of short molecules can occur during DNA extraction and present an improved silica-based extraction protocol that enables their efficient retrieval. In combination with single-stranded DNA library preparation, this method enabled us to reconstruct the mitochondrial genome sequence from a Middle Pleistocene cave bear (*Ursus deningeri*) bone excavated at Sima de los Huesos in the Sierra de Atapuerca, Spain. Phylogenetic reconstructions indicate that the *U. deningeri* sequence forms an early diverging sister lineage to all Western European Late Pleistocene cave bears. Our results prove that authentic ancient DNA can be preserved for hundreds of thousand years outside of permafrost. Moreover, the techniques presented enable the retrieval of phylogenetically informative sequences from samples in which virtually all DNA is diminished to fragments shorter than 50 bp.

Trace amounts of DNA can occasionally survive the decomposition of organic matter for long periods of time after the death of an organism. However, the retrieval of these ancient DNA molecules is severely impeded by their small size. DNA fragmentation is at least partly driven by depurination (1, 2), a continually occurring process. It is thus predicted that the degree of DNA fragmentation increases with sample age. This correlation has, in fact, been established in a recent study that analyzed samples of different ages from the same archeological sites (3), but the correlation vanishes in comparisons across different sites (4). The important role of environmental conditions, especially temperature, in DNA preservation is well recognized and reflected—for example, in the concept of thermal age (5). Unsurprisingly, permafrost environments have yielded the oldest credible records of DNA survival, including short stretches of plant and invertebrate DNA with an estimated age of up to 800,000 y that were amplified by PCR from Arctic ice cores (6, 7) and the genome sequence of a 700,000-y-old horse published recently (8). More temperate environments have yielded many DNA sequences from the Holocene and the Late Pleistocene, some as old as ~100,000 (9) or ~120,000 y (10), but only a single study has convincingly raised the possibility of DNA survival extending far into the Middle Pleistocene outside of permafrost (11). In this study, short PCR products of ~50 bp were retrieved from several bone samples of Middle Pleistocene cave bears from European caves, the oldest coming from the site of Sima de los Huesos (Atapuerca, Spain) and estimated to be >300,000 y old.

It is important to note that direct PCR amplification provides limited power to reconstruct sequences from short DNA fragments, because only fragments that are long enough to allow for

the hybridization of two PCR primers around a stretch of informative sequence are amenable to direct amplification and sequencing. If, as in the study above (11), amplicon size is decreased to ~50 bp, only ~10 bp of informative sequence remain between the priming sites, which compromises the security of sequence identification while at best allowing genotyping of single nucleotide polymorphisms. In contrast, with current library-based techniques, even shorter DNA fragments can, in principle, be sequenced in their entirety because the priming sites required for amplification and sequencing are added externally by attaching artificial adaptor sequences to the molecule ends. As an additional benefit, this approach allows the determination of damage patterns unique to ancient molecules, thus providing a framework for verifying the authenticity of ancient sequences (4, 12).

The preparation of DNA libraries and high-throughput sequencing have, without doubt, greatly advanced the scope of sequence retrieval from ancient DNA in recent years, as is documented by the generation of entire genome sequences (e.g., refs. 8 and 13–17). However, the possibility remains that not all sequence information residing in ancient specimens is optimally recovered with these methods. This possibility becomes apparent when inspecting the size distributions of sequences reported from ancient DNA (e.g., refs. 3, 8, and 15), which consistently show a mode of ~40 bp or larger. It is unclear whether the deficit

## Significance

Outside of permafrost, no contiguous DNA sequences have been generated from material older than ~120,000 y. By improving our ability to sequence very short DNA fragments, we have recovered the mitochondrial genome sequence of a >300,000-y-old cave bear from Sima de los Huesos, a Spanish cave site that is famous for its rich collection of Middle Pleistocene human fossils. This finding demonstrates that DNA can survive for hundreds of thousands of years outside of permafrost and opens the prospect of making more samples from this time period accessible to genetic studies.

Author contributions: J.D., S.P., and M.M. designed research; J.D., I.G., M.-T.G., A.W., and B.N. performed research; C.V., N.G., and J.-L.A. contributed new reagents/analytic tools; J.D., M.K., and M.M. analyzed data; and J.D., M.K., N.G., S.P., J.-L.A., and M.M. wrote the paper.

The authors declare no conflict of interest.

Data deposition: The sequence reported in this paper has been deposited in the GenBank database (accession no. [KF437625](https://doi.org/10.1093/seq/10.1073/pnas.1314445110)).

<sup>1</sup>To whom correspondence may be addressed. E-mail: [jesse\\_dabney@eva.mpg.de](mailto:jesse_dabney@eva.mpg.de), [paabo@eva.mpg.de](mailto:paabo@eva.mpg.de), or [mmeyer@eva.mpg.de](mailto:mmeyer@eva.mpg.de).

This article contains supporting information online at [www.pnas.org/lookup/suppl/doi:10.1073/pnas.1314445110/-DCSupplemental](http://www.pnas.org/lookup/suppl/doi:10.1073/pnas.1314445110/-DCSupplemental).

of shorter molecules is due to poor preservation in ancient biological specimens or their exclusion during sample preparation. This question is of importance because it is expected that the number of DNA fragments in an ancient sample increases exponentially as length decreases and, hence, that most information resides in very short molecules (3, 8). An obvious step in which loss of short molecules is expected to occur is in library preparation, because commonly used techniques require size-selective DNA purification to remove excess adaptor molecules after ligation. However, such purification steps are absent in a single-stranded library preparation method that was recently developed to sequence the genome of an archaic Denisovan individual to high coverage (16). A direct comparison of fragment size distributions obtained from sequencing the same DNA extracts following single- and double-stranded library preparation indeed revealed an improved recovery of short sequences with the single-stranded method, but Denisovan sequences of <40 bp still remained underrepresented (16).

Here we present improvements to a widely used silica-based DNA extraction technique (18) that, in combination with single-stranded library preparation, allows ancient DNA molecules as short as 30 bp to be efficiently recovered and sequenced. We describe the results from applying these methods to a bone sample of a Middle Pleistocene cave bear (*Ursus deningeri*) from Sima de los Huesos, representing the same type of material for which the longest DNA survival outside of permafrost has been proposed based on genotyping 17 mitochondrial positions where Late Pleistocene cave bears differ from brown bears (*Ursus arctos*) and American black bears (*Ursus americanus*) (11). These data support the existence of a monophyletic cave bear clade, in congruence with morphological analyses, but the exact genetic relationships within this clade remain to be determined.

## Results and Discussion

**An Improved Ancient DNA Extraction Technique.** To evaluate the efficiency at which short DNA fragments are isolated from ancient samples, we first devised a simple test assay, in which we subjected a pool of synthetic DNA fragments ranging from 35 to 150 bp to DNA extraction and measured their recovery by capillary gel electrophoresis (*SI Text, section 2*). In this experiment we focused on a single silica-based DNA extraction method, which was optimized for ancient bones and teeth by Rohland and Hofreiter (18, 19) and has been widely applied in ancient DNA studies, including, for example, the generation of the Neandertal and Denisovan genome sequences (15, 20). In brief, this method involves the following steps. First, an extraction buffer consisting of only two reagents, EDTA and proteinase K, is used to release DNA from powdered samples. DNA is then bound to silica, which is added as a suspension together with a binding buffer containing sodium acetate, sodium chloride, and guanidine thiocyanate. Finally, the silica particles with the conjugated DNA are desalted by using an ethanol wash buffer, and the DNA is eluted into a low-salt buffer. Using the test assay, we determined that the recovery of DNA fragments is indeed length-dependent, decreasing from 72% at 150 bp to only 22% at 35 bp (Fig. 1). To ameliorate this bias, we optimized the DNA extraction process with the aim of equivalently recovering DNA fragments of all sizes. This goal was achieved by the following modifications to the original protocol: (i) the use of a binding buffer containing guanidine hydrochloride, sodium acetate, and isopropanol; (ii) an increase in the volume of binding buffer relative to that of extraction buffer; and (iii) the replacement of silica suspension with commercially available silica spin columns with a custom-adapted extension reservoir to enable large loading volumes (*SI Text, section 3*).

**DNA Sequence Generation.** Using the optimized DNA extraction protocol, we generated DNA extracts from the *U. deningeri*

sample (*SI Text, section 1*) and converted them into Illumina sequencing libraries using the single-stranded library preparation method (21). To determine the size distribution of the extracted DNA fragments, we first performed shallow shotgun sequencing for a subset of the libraries. The size distribution indeed indicates highly efficient recovery of DNA fragments  $\geq 30$  bp (Fig. 2A). Because none of the sequences aligned to the mitochondrial genome of bear, we enriched the sequencing libraries for mitochondrial sequences using hybridization capture (22, 23). Temperatures of the hybridization reaction and posthybridization wash steps were lowered to facilitate the annealing of short library molecules to the probes (*SI Text, section 4*). Of the sequences obtained from the enriched libraries, only a relatively small proportion ( $\sim 4\%$ ) aligned to the published mitochondrial genome sequence of a Late Pleistocene cave bear (24) (*SI Text, section 5*, and *Dataset S1*), presumably due to the lowered stringency of hybridization enrichment. Nonetheless, after duplicate removal, 19,576 uniquely mapped sequences of a length  $\geq 30$  bp were retained and analyzed further (*Dataset S1*). Strikingly, despite a bias toward hybridizing longer molecules (Fig. S1), 94% of the sequences are no longer than 50 bp and 76% are no longer than 40 bp, respectively (Fig. 2A). The vast majority of sequenced DNA fragments are thus in a size range that was not efficiently recovered with previous methods.

**Damage Patterns.** Given the extraordinary age of the fossil ( $>300,000$  ka), cytosine deamination is expected to have converted a large proportion of terminal cytosines to uracils (4, 8). The frequency of this conversion can be approximated as the fraction of sequences that carry a T at positions where the reference sequence carries a C. In fact, we find that 62% of terminal cytosines are deaminated to uracils at the 5' end and 66% at the 3' end, respectively (Fig. 2B). These numbers are higher than those reported from other cave samples (e.g., refs. 4 and 16), and even exceed the theoretical maximum of 50% that is predicted by a model where cytosine deamination occurs predominantly in single-stranded overhangs (2). However, this excess may be explained by a bias in the sampling of sequences. DNA strands with overhangs on both ends, which are on average longer, are more likely to be recovered in hybridization capture and to pass the length threshold of 30 bp. Another observation arising from this analysis is a noticeable asymmetry in the frequency of C > T substitutions between 5' and 3' ends. Because this pattern extends from the terminal positions into the interior of the sequence, it is unlikely to be the result of biases in library preparation but may indicate that 3' overhangs are on average longer in ancient DNA. Upon reexamination, the same asymmetry, albeit less pronounced, is also observed with Denisovan (16) and Neandertal (21) sequences that were generated with the single-stranded library preparation method. Last, an analysis of DNA fragmentation patterns, which are inferred from the reference base composition around alignment start and end points, confirms previous observations (Fig. 2C). These include an elevation of G and A bases immediately adjacent to the aligned sequenced, a pattern thought to reflect strand breaks caused by depurination (2, 4, 25), as well as an excess of T bases at the first and last positions of the sequences, a pattern for which no satisfying explanation exists (2, 16).

**Mitochondrial Sequence Assembly.** Based on the raw sequence alignments, average coverage of the mitochondrial genome is 45 (Fig. S2). However, upon inspection of the alignments, we found that some regions are covered by more than one sequence variant. BLAST searches (26) of these variants revealed the presence of contaminant sequences from human, bat, corynebacteria, and, in smaller numbers, pig and fox. We therefore eliminated all sequences showing a better alignment to any of these contaminant genomes than to cave bear (8.1% of the data). After masking damage-derived Ts from the first and last three bases of each sequence (*SI Text, section 6*), a consensus was called for all

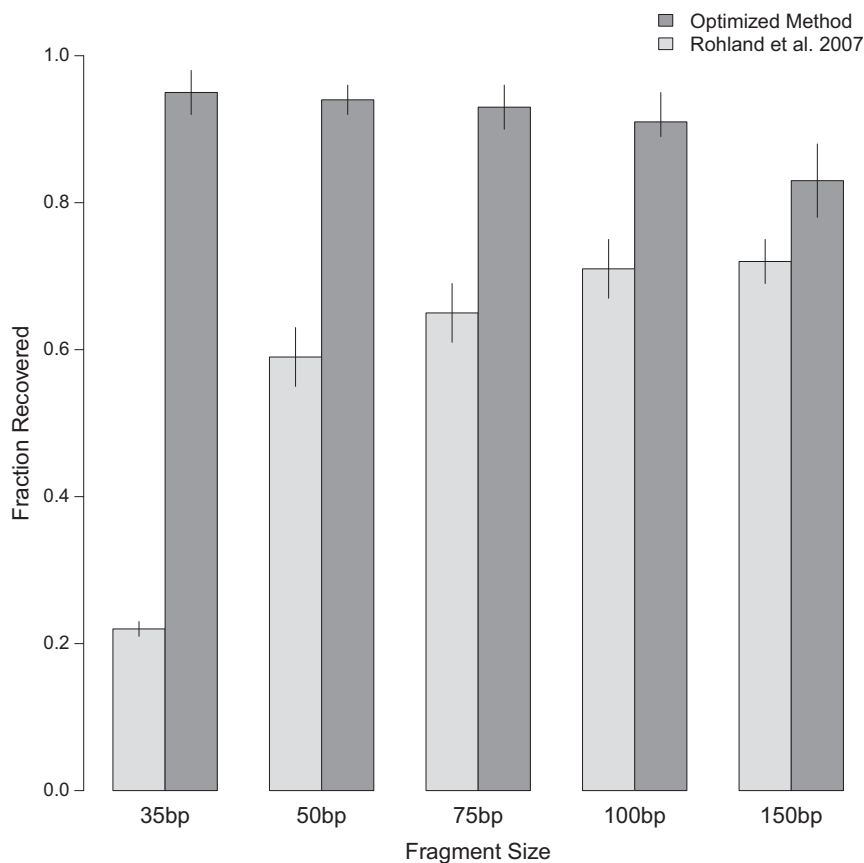


**Fig. 1.** Fragment size recovery in DNA extraction. A constructed DNA ladder of sizes relevant to ancient DNA was run through a previously published extraction method ( $n = 2$ ), as well as the current, optimized method ( $n = 4$ ). Recovered DNA was then quantified against a control ladder. Error bars represent one standard deviation.

positions where  $\geq 80\%$  of the sequences agreed and coverage was at least two. For some positions with lower consensus support, manual consensus calls were made where justifiable (Table S1). The final consensus sequence covers 16,305 bp of the cave bear mitochondrial genome. Most of the missing sequence information ( $\sim 480$  bp) is in the D loop, including a  $\sim 320$ -bp stretch of repetitive sequence that cannot be resolved with short sequences. Outside the D loop, only five positions remain undetermined.

**Phylogenetic Position of *U. deningeri*.** The earliest fossil evidence of cave bear-derived morphological features is found  $\sim 1.2$  Ma in *Ursus dolinensis*, a species that was defined in Atapuerca Gran Dolina (TD4) (27) but is also recorded at Atapuerca Trincheras Elefante (TE9) (28) and Untermassfeld (29, 30). An abundant fossil record in Europe and parts of Asia indicates that subsequent cave bear evolution proceeded through the Middle Pleistocene form *U. deningeri*, which transitioned into the Late Pleistocene form *Ursus spelaeus sensu lato* (31), before cave bears went extinct 28 ka (32). Genetic and morphological analyses support a further differentiation of three types of Late Pleistocene cave bears. The first two, *U. spelaeus sensu stricto* and *Ursus ingressus*, are predominantly found in Europe and are thought to have become reproductively isolated (33). The third type has been found only in the Caucasus and the Yana river region in Eastern Siberia and was designated *U. deningeri kudarensis* (34) based on its more ancestral dental morphology. It also shows a divergent mitochondrial haplotype (35, 36).

After aligning the sequence of the Sima de los Huesos specimen, which is considered a typical representative of Middle Pleistocene *U. deningeri* based on skeletal morphology (31), to published mitochondrial genome sequences of Late Pleistocene cave bears (24, 36, 37), we used a maximum-likelihood (ML) approach to reconstruct the phylogenetic relationships among

cave bears (SI Text, section 7). The *U. deningeri* lineage branches off basal to the common ancestor of *U. spelaeus s.s.* and *U. ingressus* with good statistical support (Fig. 3), a result that is in line with morphological analyses. It is noteworthy, however, that the Sima de los Huesos sequence is located on a branch of substantial length. Sequences from additional specimens will therefore be needed to determine how closely the Sima de los Huesos population is related to the *U. deningeri* population that gave rise to Late Pleistocene cave bears. Interestingly, Late Pleistocene *U. deningeri kudarensis* from the Caucasus remain the most divergent cave bear lineage, further supporting the hypothesis that they may represent a separate branch of cave bear evolution.

As expected due to its Middle Pleistocene origin, the cave bear sequence from Sima de los Huesos exhibits a shorter branch than any of the Late Pleistocene sequences in the tree. Combined ESR and U-series dating of two sets of cave bear bones from Sima de los Huesos have previously suggested minimum ages of 200 ka for one set and 300 ka for the other (38), but based on the macro- and microfaunal associations, an age  $>300$  ka seems very likely for all bears in the site (39). We attempted molecular dating of the fossil via tip calibration (40) using the radio-carbon and stratigraphic dates associated with 14 of the Late Pleistocene cave bear sequences (SI Text, section 8), yielding an age estimate of 409 ka, but with poor resolution (95% confidence interval: 179–680 ka). It should also be noted that the bear sample analyzed here was found in a layer that contained hominin remains. For these, an age  $>530$  ka has been suggested based on geological analyses (41). However, the age of the Sima de los Huesos fossils is currently being re-evaluated using additional geological data, work that will be important especially for interpreting the human fossil record.

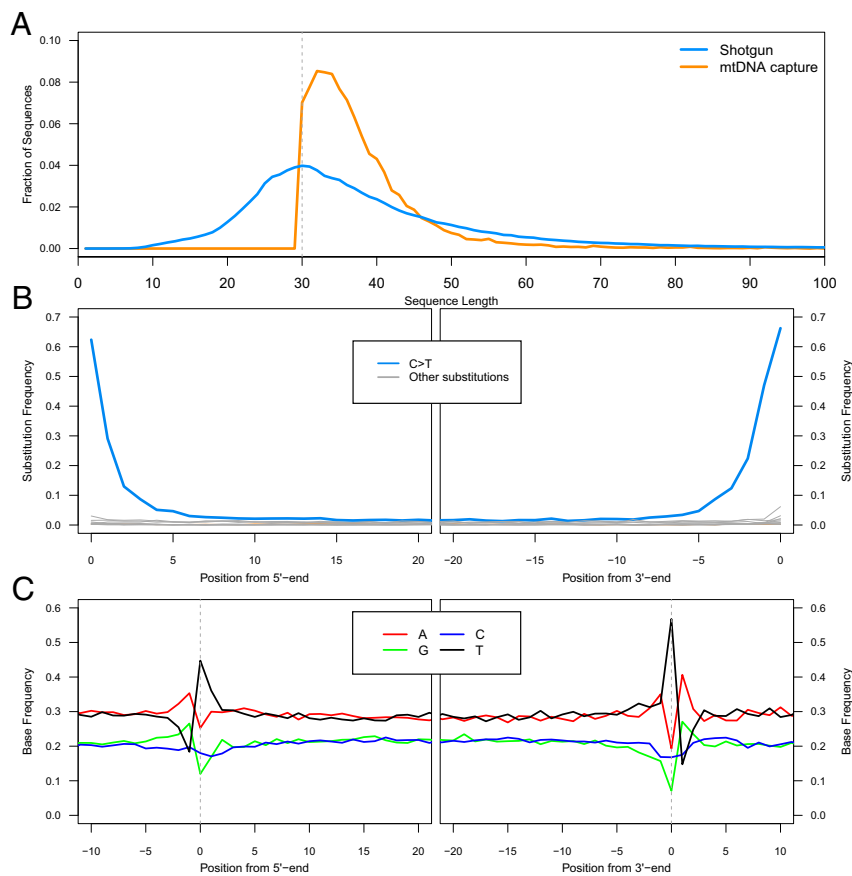


**Fig. 2.** Length distributions and damage patterns. (A) Fragment length distributions of shotgun sequences (blue) and captured mitochondrial sequences (orange) as the fraction of sequences in each size bin. (B) Substitution patterns at the 5' and 3' ends of the aligned sequences. (C) DNA fragmentation patterns inferred from the reference base composition around alignment start and end points.

## Conclusion

We demonstrate that very short ancient DNA fragments can be efficiently extracted and sequenced and can be used for the reconstruction of contiguous, phylogenetically informative DNA sequences. The strong signal of cytosine deamination, the short size of the DNA fragments, and the unique positioning of the sample in the phylogenetic tree provide multiple lines of evidence for the authenticity of the mitochondrial genome sequence from the Sima de los Huesos cave bear, confirming that DNA can indeed survive for hundreds of thousands of years outside of permafrost (11), albeit in an extremely fragmentary state.

We note that, although the vast majority of cave bear sequences are only 30–50 bp in length, we have not yet systematically explored the lower size limit of DNA fragments surviving in ancient bone. It is therefore possible that even shorter molecules can be made available for sequencing in the future, by using library-based techniques as described here or directly via single-molecule sequencing (8, 25). However, in addition to further optimizations of the DNA extraction method, such attempts will have to include improvements to hybridization enrichment of very short molecules and the development of new sequence analysis strategies that allow for confidently aligning very short sequences to a reference genome while discriminating endogenous sequences from contaminating environmental DNA. We hope that the methodology presented here will help to retrieve ancient DNA sequences from additional organisms of the Middle Pleistocene period. The fossil remains from Sima de los Huesos will undoubtedly remain in the focus of such efforts,

because they include the largest assembly of Middle Pleistocene hominin fossils in the world (42).

## Materials and Methods

**Sampling, DNA Extraction, and Library Preparation.** By using a dentistry drill, 1.8 g of fine powder were obtained from an *U. deningeri* radius (SH-01-S16-38) from Sima de los Huesos. From this powder, 19 DNA extracts were generated with the optimized extraction protocol presented here (*SI Text, section 3*), aliquots of which were converted into 23 DNA libraries (21). In addition, three blank controls were added during both DNA extraction and library preparation and were carried alongside the sample libraries through all subsequent steps. Libraries were amplified by PCR using AccuPrime Pfx DNA polymerase (Life Technologies) (43) following a double-indexing scheme described elsewhere (44).

**Enrichment, Sequencing, and Assembly of the Mitochondrial Genome.** Mitochondrial DNA was enriched in successive experiments by capture with three different probe sets (*SI Text, section 4*). Briefly, the first experiment was performed by using biotinylated PCR products as probes, which were derived from amplifying the brown bear mitochondrial genome in overlapping fragments of ~2,000 bp. To minimize sequence divergence between sample and probes, we subsequently generated a second set of shorter probes (250–300 bp) using DNA from a Late Pleistocene cave bear specimen with very good DNA preservation (24). Last, we designed a set of biotinylated oligonucleotides to close gaps in the assembly remaining after enrichment with the brown and cave bear probes. Enriched libraries were sequenced on a total of 5 MiSeq lanes (Illumina) by using recipes for double-indexed paired-end sequencing (44). Full-length molecule sequences were generated from overlapping forward and reverse sequence reads (45). Unmerged reads and those that did not perfectly match one of the expected index combinations were discarded. The remaining sequences were aligned against a published mitochondrial genome



1. Lindahl T (1993) Instability and decay of the primary structure of DNA. *Nature* 362(6422):709–715.
2. Briggs AW, et al. (2007) Patterns of damage in genomic DNA sequences from a Neandertal. *Proc Natl Acad Sci USA* 104(37):14616–14621.
3. Allentoft ME, et al. (2012) The half-life of DNA in bone: Measuring decay kinetics in 158 dated fossils. *Proc Biol Sci* 279(1748):4724–4733.
4. Sawyer S, Krause J, Guschanski K, Savolainen V, Pääbo S (2012) Temporal patterns of nucleotide misincorporations and DNA fragmentation in ancient DNA. *PLoS ONE* 7(3): e34131.
5. Smith CI, Chamberlain AT, Riley MS, Stringer C, Collins MJ (2003) The thermal history of human fossils and the likelihood of successful DNA amplification. *J Hum Evol* 45(3): 203–217.
6. Willerslev E, et al. (2003) Diverse plant and animal genetic records from Holocene and Pleistocene sediments. *Science* 300(5620):791–795.
7. Willerslev E, et al. (2007) Ancient biomolecules from deep ice cores reveal a forested southern Greenland. *Science* 317(5834):111–114.
8. Orlando L, et al. (2013) Recalibrating Equus evolution using the genome sequence of an early Middle Pleistocene horse. *Nature* 499(7456):74–78.
9. Orlando L, et al. (2006) Revisiting Neandertal diversity with a 100,000 year old mtDNA sequence. *Curr Biol* 16(11):R400–R402.
10. Lindqvist C, et al. (2010) Complete mitochondrial genome of a Pleistocene jawbone unveils the origin of polar bear. *Proc Natl Acad Sci USA* 107(11):5053–5057.
11. Valdiosera C, et al. (2006) Typing single polymorphic nucleotides in mitochondrial DNA as a way to access Middle Pleistocene DNA. *Biol Lett* 2(4):601–603.
12. Krause J, et al. (2010) A complete mtDNA genome of an early modern human from Kostenki, Russia. *Curr Biol* 20(3):231–236.
13. Miller W, et al. (2008) Sequencing the nuclear genome of the extinct woolly mammoth. *Nature* 456(7220):387–390.
14. Rasmussen M, et al. (2010) Ancient human genome sequence of an extinct Palaeo-Eskimo. *Nature* 463(7282):757–762.
15. Green RE, et al. (2010) A draft sequence of the Neandertal genome. *Science* 328(5979):710–722.
16. Meyer M, et al. (2012) A high-coverage genome sequence from an archaic Denisovan individual. *Science* 338(6104):222–226.
17. Keller A, et al. (2012) New insights into the Tyrolean Iceman's origin and phenotype as inferred by whole-genome sequencing. *Nat Commun* 3:698.
18. Rohland N, Hofreiter M (2007) Ancient DNA extraction from bones and teeth. *Nat Protoc* 2(7):1756–1762.
19. Rohland N, Hofreiter M (2007) Comparison and optimization of ancient DNA extraction. *Biotechniques* 42(3):343–352.
20. Reich D, et al. (2010) Genetic history of an archaic hominin group from Denisova Cave in Siberia. *Nature* 468(7327):1053–1060.
21. Gansauge MT, Meyer M (2013) Single-stranded DNA library preparation for the sequencing of ancient or damaged DNA. *Nat Protoc* 8(4):737–748.
22. Maricic T, Whitten M, Pääbo S (2010) Multiplexed DNA sequence capture of mitochondrial genomes using PCR products. *PLoS ONE* 5(11):e14004.
23. Fu Q, et al. (2013) DNA analysis of an early modern human from Tianyuan Cave, China. *Proc Natl Acad Sci USA* 110(6):2223–2227.
24. Krause J, et al. (2008) Mitochondrial genomes reveal an explosive radiation of extinct and extant bears near the Miocene-Pliocene boundary. *BMC Evol Biol* 8:220.
25. Orlando L, et al. (2011) True single-molecule DNA sequencing of a pleistocene horse bone. *Genome Res* 21(10):1705–1719.
26. Altschul SF, et al. (1997) Gapped BLAST and PSI-BLAST: A new generation of protein database search programs. *Nucleic Acids Res* 25(17):3389–3402.
27. García N, Arsuaga JL (2001) *Ursus dolinensis*: A new species of early pleistocene ursid from Trinchera Dolina, Atapuerca (Spain). *Cr Acad Sci II A* 332(11):717–725.
28. Carbonell E, et al. (2008) The first hominin of Europe. *Nature* 452(7186):465–469.
29. García N (2004) New results on the remains of Ursidae from Untermassfeld: Comparisons with *Ursus dolinensis* from Atapuerca and other early and middle Pleistocene sites. *Late Neogene and Quaternary Biodiversity and Evolution: Regional Developments and Interregional Correlations Conference*, 18th International Senckenberg Conference, Weimar, Germany, eds Kahlke R-D, Maul LC, Mazza PP (Terra Nostra, Schriften der Alfred-Wegener-Stiftung, Berlin), pp 112–113.
30. Kahlke R-D (2006) *Untermassfeld: A Late Early Pleistocene (Epivillafranchian) Fossil Site Near Meiningen (Thuringia, Germany) and its Position in the Development of the European Mammal Fauna* (Archaeopress, Oxford).
31. García N, Arsuaga JL, Torres T (1997) The carnivore remains from the Sima de los Huesos Middle Pleistocene site (Sierra de Atapuerca, Spain). *J Hum Evol* 33(2-3): 155–174.
32. Pacher M, Stuart AJ (2009) Extinction chronology and palaeobiology of the cave bear (*Ursus spelaeus*). *Boreas* 38(2):189–206.
33. Hofreiter M, et al. (2004) Evidence for reproductive isolation between cave bear populations. *Curr Biol* 14(1):40–43.
34. Baryshnikov G (1998) Cave bears from the Paleolithic of the Greater Caucasus. *Quaternary Paleozoology in the Northern Hemisphere*, eds Saunders JJ, Styles BV, Baryshnikov GF (Illinois State Museum, Springfield, IL), pp 69–118.
35. Knapp M, et al. (2009) First DNA sequences from Asian cave bear fossils reveal deep divergences and complex phylogeographic patterns. *Mol Ecol* 18(6):1225–1238.
36. Stiller M, Knapp M, Stenzel U, Hofreiter M, Meyer M (2009) Direct multiplex sequencing (DMPS)—a novel method for targeted high-throughput sequencing of ancient and highly degraded DNA. *Genome Res* 19(10):1843–1848.
37. Bon C, et al. (2008) Deciphering the complete mitochondrial genome and phylogeny of the extinct cave bear in the Paleolithic painted cave of Chauvet. *Proc Natl Acad Sci USA* 105(45):17447–17452.
38. Bischoff JL, et al. (1997) Geology and preliminary dating of the hominid-bearing sedimentary fill of the Sima de los Huesos Chamber, Cueva Mayor of the Sierra de Atapuerca, Burgos, Spain. *J Hum Evol* 33(2-3):129–154.
39. García N, Arsuaga JL (2011) The Sima de los Huesos (Burgos, northern Spain): Palaeoenvironment and habitats of *Homo heidelbergensis* during the Middle Pleistocene. *Quat Sci Rev* 30(11-12):1413–1419.
40. Shapiro B, et al. (2011) A Bayesian phylogenetic method to estimate unknown sequence ages. *Mol Biol Evol* 28(2):879–887.
41. Bischoff JL, et al. (2007) High-resolution U-series dates from the Sima de los Huesos hominids yields: Implications for the evolution of the early Neandertal lineage. *J Archaeol Sci* 34(5):763–770.
42. Arsuaga JL, et al. (1997) Sima de los Huesos (Sierra de Atapuerca, Spain). The site. *J Hum Evol* 33(2-3):109–127.
43. Dabney J, Meyer M (2012) Length and GC-biases during sequencing library amplification: A comparison of various polymerase-buffer systems with ancient and modern DNA sequencing libraries. *Biotechniques* 52(2):87–94.
44. Kircher M, Sawyer S, Meyer M (2012) Double indexing overcomes inaccuracies in multiplex sequencing on the Illumina platform. *Nucleic Acids Res* 40(1):e3.
45. Kircher M, Heyn P, Kelso J (2011) Addressing challenges in the production and analysis of Illumina sequencing data. *BMC Genomics* 12:382.
46. Li H, Durbin R (2009) Fast and accurate short read alignment with Burrows-Wheeler transform. *Bioinformatics* 25(14):1754–1760.
47. Kircher M (2012) Analysis of high-throughput ancient DNA sequencing data. *Methods Mol Biol* 840:197–228.
48. Katoh K, Standley DM (2013) MAFFT multiple sequence alignment software version 7: Improvements in performance and usability. *Mol Biol Evol* 30(4):772–780.
49. Keis M (2013) Brown bear (*Ursus arctos*) phylogeography in northern Eurasia. Doctoral dissertation (Univ of Tartu, Tartu, Estonia).

# Supporting Information

Dabney et al. 10.1073/pnas.1314445110

## SI Text

**1. Sample Information.** The Sima de los Huesos is a well-known site that has provided the largest collection of Middle Pleistocene hominin fossils (1–5). It is located deep inside a large karst system (Cueva Mayor) and approximately half a kilometer from the present-day entrance. In deep caves, temperatures do not oscillate during the year and are coincident with the annual average temperature outside the cave. In glacial periods, the average temperature dropped in the Central Plateau of Spain by ~5 °C. Measurements taken in the Galeria del Silex, another gallery of the Cueva Mayor, indicate a fairly constant temperature of 10.6 °C and humidity >99% (6). The clays containing the bear fossil (SH01-S16-38) used in this study are wet and have never dried out due to the environmental conditions having remained very consistent throughout the cave system.

The bear fossil sampled was excavated in the 2001 field season. It is a complete radius, which was recovered broken into two adjoining parts that were in close spatial proximity. The fossil was found in the same layer (Upper Red Clays) that contains the hominin fossils. In the excavation square (S16) of the bear radius, two hominin fossils (a femur and a humerus) were also recovered. After excavation, the bear radius was left to dry in the field laboratory, then washed in water and dried before storing. No chemicals were used for preservation.

**2. Testing Improvements to DNA Extraction Method.** To test the performance of the extraction protocol in recovering DNA molecules of relevant sizes to ancient DNA studies, we constructed a DNA ladder by pooling 35-, 50-, 75-, 100-, and 150-bp NoLimit DNA fragments (ThermoScientific). To mimic the conditions of the initial step of DNA extraction from actual samples, for each extraction an aliquot of 285 ng of DNA ladder in a volume of 50  $\mu$ L was added to 1 mL of extraction buffer (0.45 M EDTA, 0.25 mg/mL Proteinase K, pH 8.0) (7, 8). This solution was then added to the following: (i) 4 mL of a 5 M guanidine thiocyanate, 0.3 M sodium acetate binding buffer (pH 4.5), and 100  $\mu$ L of silica suspension, whereupon extraction was completed according to a previous protocol (8); or (ii) 10.5 mL of a binding buffer containing 5 M guanidine hydrochloride, 40% (vol/vol) isopropanol, 0.05% Tween-20, and 90 mM sodium acetate (pH 5.2), after which extraction was completed as described in *SI Text*, section 3, except that two 25- $\mu$ L TET buffer (10 mM Tris-HCl, 1 mM EDTA, 0.05% Tween-20, pH 8.0) aliquots were used for elution. Quantification of each extract and the control ladder was performed on a BioAnalyzer 2100 (Agilent) by using a DNA 1000 chip. The efficiency of recovery for each fragment was calculated by dividing the concentration of DNA in the extract by that of the control ladder.

**3. DNA Extraction and Library Preparation.** Approximately 1.8 g of bone was drilled into a fine powder with a dental drill. Between 85 and 120 mg of bone powder went into each of 19 extractions along with 1 mL of extraction buffer (final concentrations: 0.45 M EDTA, 0.25 mg/mL Proteinase K, pH 8.0). The bone powder was resuspended by vortexing, and the suspension was rotated at 37 °C overnight (~18 h) (8). Remaining bone powder was then pelleted by centrifugation in a bench-top centrifuge for 2 min at maximum speed (16,100  $\times$  g). The supernatant was added to 13 mL of binding buffer containing, in final concentrations, 5 M guanidine hydrochloride, 40% (vol/vol) isopropanol, 0.05% Tween-20, and 90 mM sodium acetate (pH 5.2). A binding apparatus was constructed by forcefully fitting an extension res-

ervoir removed from a Zymo-Spin V column (Zymo Research), which had been submerged in a bleach bath for 20 min, rinsed with water, and UV irradiated before use, into a MinElute silica spin column (Qiagen). The extension reservoir-MinElute assembly was then placed into a 50-mL falcon tube. The 14-mL solution containing binding buffer and the extraction supernatant was then poured into the extension reservoir, and the falcon tube cap was secured. The binding apparatus was centrifuged for 4 min at 1,500  $\times$  g, rotated 90°, and centrifuged for an additional 2 min at the same speed. The extension reservoir-MinElute column were removed from the falcon tube and placed into a clean 2-mL collection tube. The extension reservoir was removed, and the MinElute column was dry-spun for 1 min at 6,000 rpm (3,300  $\times$  g) in a bench-top centrifuge. Two wash steps were performed by adding 750  $\mu$ L of PE buffer (Qiagen) to the MinElute column, centrifuging at 3,300  $\times$  g and discarding the flow-through. The column was dry-spun for 1 min at maximum speed (16,100  $\times$  g) and then placed in a fresh 1.5-mL collection tube. For elution, 12.5  $\mu$ L of TET buffer was pipetted onto the silica membrane, and after a 2- to 5-min incubation was collected by centrifugation for 30 s at maximum speed. This step was repeated for a total of 25  $\mu$ L of DNA extract.

A total of 23 single-stranded libraries were prepared by using up all sample extracts (9). Each library was amplified into PCR plateau by using two uniquely barcoded primers (10) as described elsewhere (9). The amplified libraries were then quantified on a NanoDrop ND-1000 (Nanodrop Technologies). A subset of three libraries was included for shallow shotgun sequencing on 10% of a MiSeq lane (Illumina) dedicated to another project. Sequencing, filtering, and mapping were performed as described in *SI Text*, section 4. Of 931,307 merged sequences, none aligned to the cave bear mitochondrial genome.

**4. Mitochondrial Capture and Sequencing.** Mitochondrial captures were performed by using three probe sets: *Ursus arctos* (brown bear) probes, *Ursus spelaeus* (cave bear) probes, and synthetic oligonucleotide probes. Brown bear probes were prepared by amplifying brown bear mitochondrial DNA in 9 overlapping fragments of ~2 kb. These PCR products were then converted into biotinylated capture probes as described in Maricic et al. (11). Cave bear probes were prepared by using the bone SP891 from which the published *U. spelaeus* mitochondrial genome is derived (12) and a multiplex PCR approach (13). PCR primers were designed by using Primer3 (14) and the published *U. spelaeus* mitochondrial genome (NC\_011112.1) to amplify 80 regions of 250–300 bp tiled across the genome. One of the primers in each pair was synthesized with a 5' biotin. Dilutions were made of an existing extract from SP891 and used as template in a two-step multiplex PCR approach as published (13, 15). Final PCR products were purified with solid-phase reversible immobilization (SPRI) beads and quantified on a NanoDrop ND-1000 photospectrometer. The 80 purified amplicons were then pooled in equal ratios and used as capture probes. The 5' biotinylated synthetic oligonucleotides were designed to cover gaps in the initial sequence alignment of libraries captured with brown and cave bear baits. A total of 39 oligonucleotides of length 50–71 bp spanning these gaps were created by using an alignment of all published *U. spelaeus* mitochondrial sequences and the *U. arctos* mitochondrial sequence. Wobble bases in the oligonucleotides were allowed at polymorphic positions to increase the likelihood of recovery. The oligonucleotides were pooled in equimolar ratios and used as capture probes.

Two serial captures were performed by using 2  $\mu$ g of each library as input according to the protocol provided in Maricic et al. (11) for the brown bear and cave bear probe sets and Fu et al. (16) for the oligonucleotide probe set. Hybridization and posthybridization wash temperatures were decreased to 60 °C and 57 °C, respectively, for both protocols. After the first round of capture, enriched libraries were amplified for 30 cycles in 100- $\mu$ L reactions by using Herculase II Fusion polymerase (Agilent) (17) and the primer pair IS5/IS6 (18). The amplified libraries were quantified on a NanoDrop, and 500 ng of each were used as input for the second round of capture. Amplified postcapture libraries from this round were quantified on a NanoDrop and pooled in equal amounts. This pool of serial captured libraries was then amplified in a one-cycle reconditioning PCR (50  $\mu$ L of Herculase II Fusion reactions) to remove heteroduplicates and quantified on a DNA 1000 chip (Agilent) for sequencing. All library pools were sequenced on 76 cycle paired-end runs with two index reads (10) on Illumina's MiSeq platform.

**5. Raw Sequence Processing, Mapping, and Removal of Duplicates.** All sequences from the three different hybridization enrichment experiments were combined and analyzed jointly. Base calling was performed by using Illumina's Bustard software, and the index reads were used to split sequences into separate files for each indexed source library. Sequences that did not perfectly match one of the expected index combinations were excluded from further analysis. To reconstruct full-length molecule sequences, forward and reverse reads were merged into single sequences if they overlapped by at least 11 bp (19). Nonmerged sequences and sequences <30 bp were discarded. All other sequences were aligned against a published mitochondrial genome sequence of a Late Pleistocene cave bear (NC\_011112.1) by using BWA (20). Because BWA does not account for the circularity of the mitochondrial genome, 500 bp of sequence were moved from the beginning of the reference genome sequence to its end. After this rearrangement, both ends of the reference sequence were located within a ~320-bp stretch of repetitive sequence in the D loop, which cannot be resolved by mapping of short sequence reads. Alignment parameters were chosen as follows: (i) “-n 5” to allow for up to five mismatches (with default parameters five mismatches are only accepted for sequences of at least 93 bp); (ii) “-o 1” (BWA default) to allow for 1 insertion/deletion; and (iii) “-I 16500” to turn off the seeding. Less stringent alignment parameters were chosen to prevent the loss of sequences of ancient DNA fragments with multiple deoxyuracils. After mapping, duplicate sequences were removed by calling a consensus from sequences with identical start and end coordinate (21). On average, each unique fragment was represented by 102 sequences. All BAM files containing the unique sequences of each sample library were then merged into a single file. Sequences with a map quality score <30 (~6% of the sequences) were excluded from further analysis to ensure unique placement of all sequences within the mitochondrial genome.

Dataset S1 shows the number of unique sequences obtained from each indexed library after hybridization enrichment with three different probe sets. All sequences derived from extraction or library preparation controls were subjected to a BLAST search. Most could be identified as human contaminants, but six produced a best match to bear mitochondrial DNA. Notably, despite the large average number of duplicate sequences obtained from each DNA fragment, each of these sequences was observed only once. When searching for identical sequences in the sample libraries, we found that all were present in between 25 and 12,484 duplicates in one other library, indicating that they result from cross-contamination among libraries rather than from contamination with exogenous bear DNA. Low levels of cross-contamination are, for example, introduced by multiplex sequencing, where sequences are occasionally assigned to the wrong sample (10).

From the sample libraries, a total of 19,576 unique sequences could be aligned against the cave bear mitochondrial genome (derived from 2,025,774 sequences before uniqueness filtering). Average unique coverage across the mitochondrial genome is 45-fold. All positions in the mitochondrial genome are covered by at least two sequences, except for two very short regions (25 and 41 bp) and a repetitive sequence stretch within the D loop, as well as 3 bp outside the D loop that were covered only once (Fig. S2).

**6. Consensus Calling.** Using the “tview” option of the samtools software package (22), we first visually inspected the sequence alignments to the cave bear mitochondrial reference genome and identified several small regions where more than one sequence variant was present. We performed BLAST searches using subsets of sequences in such regions and retrieved either best matches to bear mtDNA or one of the following types of sequences: human mtDNA, mtDNA of several bat species, pig mtDNA, fox mtDNA, and corynebacteria ulcerans DNA. The occurrence of such environmental contaminants is not surprising, despite the fact that bear DNA sequences were used in hybridization enrichment of the DNA libraries, because some regions in the mammalian mitochondrial genome are highly conserved and differ only little between very distantly related species.

To remove most of the contaminant sequences without extensive manual editing of the alignment file, we aligned all sequences against the following set of putative contaminant genomes using BWA and the alignment parameters indicated earlier: the human genome (hg19/1000G), all 37 complete mtDNA genomes of bats (taxonomic order Chiroptera; txid9397) available in GenBank, a fox (*Vulpes vulpes*) mtDNA genome (AM181037.1), a pig (*Sus scrofa*) mtDNA genome (AF034253.1), and the complete genome of corynebacteria ulcerans 0102 (AP012284.1). We then removed all sequences (1,578 in total; 8% of the data) that produced a better alignment to one of the contaminant genomes than to cave bear mtDNA (more specifically, we compared the edit distance as provided in the “NM” field of the SAM/BAM format). Sequences removed by this filter were on average longer than those retained (50 vs. 38 bp, respectively), indicating a more recent origin of at least some of the contamination. Putative contaminant sequences were localized in several short regions of the mitochondrial genome, including, for example, the slowly evolving 16S rRNA gene (Fig. S2). Further, to eliminate spurious alignments while retaining sequences strongly affected by deamination, we removed sequences showing more than two mismatches other than C>T to the reference genome in the orientation they were sequenced.

To avoid false consensus calls due to damage-derived C->T changes, all T residues (or A if the sequence was aligned in reverse complementary orientation) within the first three and last three bases of each sequence were replaced by “N” in the sequence alignment file if at least one other sequence showed a C at the respective position in the alignment to the cave bear mtDNA genome. Using this filter, we assume that damage-derived substitutions in the interior of sequences are too infrequent to affect more than half of the sequences at a given alignment position with multifold coverage. For consensus calling, a tabular position-based “pileup” file was generated from the BAM alignment file using “samtools mpileup”. This file was used to call majority consensus bases at positions covered by at least two reads and to determine the proportion of reads supporting the consensus base at each position. Using the latter information, we manually inspected all positions where <80% of the sequences agreed with the consensus and corrected the consensus calls where appropriate (Table S1).

It may theoretically occur that true evolutionary changes in highly conserved regions of the mitochondrial genome are shared with one of the contaminant genomes (see above), but not the cave bear reference genome. In this case, the correct sequence variant would erroneously be identified as contamination after

mapping to the set of contaminant genomes (see above), whereas the actual contamination is enriched in the residual sequence alignment. To exclude this possibility, we inspected the raw sequence alignment at all positions where  $\geq 25\%$  of the sequences had been removed as putative contaminants before consensus calling (Fig. S2). We found that the sequence variant represented by the consensus is in all cases supported by sequences with terminal C->T substitutions (or G->A, depending on sequence orientation). This typical pattern of ancient DNA damage is absent in the putative contaminants, again indicating that the contamination is relatively recent (as expected, for example, with human and pig). Alternatively, contaminant sequences may have aligned to the cave bear reference genome due to random sequence similarity.

**7. Phylogenetic Reconstructions.** We removed all sites with ambiguities in one or more sequences from the complete mtDNA genome alignment, resulting in an alignment of 9,592 bp. We then identified the best-fitting nucleotide substitution model for this alignment with ModelTest (Version 3.7; ref. 23). The Akaike Information Criterion (AIC) supported GTR+I+ $\Gamma$  as the best-fitting model. Phylogenetic trees were reconstructed with paup (Version 4.0b10; ref. 24) under the maximum-likelihood (ML) optimality criterion. The paup-ML tree was reconstructed by using a neighbor-joining starting tree, followed by tree-bisection-and-reconnection optimization by using the parameters from the above ModelTest analyses. Subsequently, bootstrap analyses were performed with paup under the same settings as before, by using 500 bootstrap pseudoreplicates of the dataset. Bootstrap trees were summarized with a 50%-majority-rule consensus.

**8. Molecular Dating.** We estimated the age of the cave bear sample from Sima de los Huesos using the temporal information available from our cave bear samples of known age. We used a Bayesian Markov Chain Monte Carlo (MCMC) approach as described in detail by Shapiro et al. (25) and as implemented in the software Beast (Version 1.7.5; ref. 26). To reduce ambiguity in our analyses, we excluded all undated samples from the dataset and used only the 14 samples of known age (27) to estimate the age of the sample from Sima de los Huesos. The dataset was otherwise identical to the one used for the phylogenetic analyses.

Analyses were conducted in Beast (Version 1.7.5) under the HKY+I nucleotide substitution model, which was identified by

the AIC as the best-supported model for this small dataset. To constrain the tree space to be sampled by the MCMC, we limited analyses to trees in which all dated samples form a monophyletic group with respect to the sample from Sima de los Huesos, a topology consistent with the most well-supported phylogeny identified in the analyses described above (Fig. 3). Furthermore, we introduced a normally distributed prior for the substitution rate of  $3.485 \times 10^{-8}$  substitutions per site per year (95% highest posterior density:  $1.525 \times 10^{-8} - 5.445 \times 10^{-8}$ ) (28). We used a uniform prior of 0–1,000,000 y for the age of the sample from Sima de los Huesos. We decided in favor of this weak prior in order to obtain an unbiased age estimate. All other priors were left at default settings. The MCMC was run for 100 million generations, sampling every 10,000 generations with a burn-in of 10 million generations. Analyses were conducted under the assumption of a strictly clocklike evolution of the cave bear mitochondrial genome as well as under a relaxed clock with lognormal distribution of nucleotide substitution rates across branches. Results were compared by using Bayes factors (BF) (29). The relaxed clock was not decisively better than the strict clock ( $\log_{10}$  BF: 0.8), with “decisive” being defined as a  $\log_{10}$  BF of  $> 2$  (29). We also evaluated a constant population size coalescent prior against a more complex Skyline Plot prior in the same way. Again, the more complex model was not decisively better than the simpler model (BF: 0.07). Using a constant size coalescent prior and a strict molecular clock model, we then repeated the age estimation analyses for the Sima de los Huesos sample three times with the settings described above. Convergence of the algorithm was checked with Tracer (Version 1.5; <http://tree.bio.ed.ac.uk/software/tracer/>). Results from the three runs were combined to provide a final estimate of the age of the Sima de los Huesos sample.

Two additional analyses were performed to test the robustness of the molecular dating result. First, using the settings described above, we sampled from the prior distribution only to identify a potential influence of our prior settings on the estimated age. No influence could be identified. Second, after removing the Sima de los Huesos sample from the alignment, we individually estimated the age of all radiocarbon-dated samples using the settings described above. Of seven tested samples, the radiocarbon age was outside the 95% highest posterior density (HPD) of the estimated age in two cases, but only by a maximum of 5,150 y (Table S2).

1. Arsuaga JL, et al. (1997) Sima de los Huesos (Sierra de Atapuerca, Spain). The site. *J Hum Evol* 33(2-3):109–127.
2. Arsuaga JL, et al. (1997) Size variation in Middle Pleistocene humans. *Science* 277(5329):1086–1088.
3. Arsuaga JL, Martínez I, Gracia A, Carretero JM, Carbonell E (1993) Three new human skulls from the Sima de los Huesos Middle Pleistocene site in Sierra de Atapuerca, Spain. *Nature* 362(6420):534–537.
4. Arsuaga JL (2010) Colloquium paper: Terrestrial apes and phylogenetic trees. *Proc Natl Acad Sci USA* 107(Suppl 2):8910–8917.
5. Arsuaga JL, et al. (1999) A complete human pelvis from the Middle Pleistocene of Spain. *Nature* 399(6733):255–258.
6. Martin-Chivelet J, et al. (2011) Land surface temperature changes in Northern Iberia since 4000yr BP, based on  $\delta^{13}C$  of speleothems. *Global Planet Change* 77:1–12.
7. Rohland N, Hofreiter M (2007) Comparison and optimization of ancient DNA extraction. *Biotechniques* 42(3):343–352.
8. Rohland N, Hofreiter M (2007) Ancient DNA extraction from bones and teeth. *Nat Protoc* 2(7):1756–1762.
9. Gansauge M-T, Meyer M (2013) Single-stranded DNA library preparation for the sequencing of ancient or damaged DNA. *Nat Protoc* 8(4):737–748.
10. Kircher M, Sawyer S, Meyer M (2012) Double indexing overcomes inaccuracies in multiplex sequencing on the Illumina platform. *Nucleic Acids Res* 40(1):e3.
11. Maricic T, Whitten M, Pääbo S (2010) Multiplexed DNA sequence capture of mitochondrial genomes using PCR products. *PLoS ONE* 5(11):e14004.
12. Krause J, et al. (2008) Mitochondrial genomes reveal an explosive radiation of extinct and extant bears near the Miocene-Pliocene boundary. *BMC Evol Biol* 8:220.
13. Krause J, et al. (2006) Multiplex amplification of the mammoth mitochondrial genome and the evolution of Elephantidae. *Nature* 439(7077):724–727.
14. Rozen S, Skaletsky H (2000) Primer3 on the WWW for general users and for biologist programmers. *Methods Mol Biol* 132:365–386.
15. Römpler H, et al. (2006) Multiplex amplification of ancient DNA. *Nat Protoc* 1(2):720–728.
16. Fu Q, et al. (2013) DNA analysis of an early modern human from Tianyuan Cave, China. *Proc Natl Acad Sci USA* 110(6):2223–2227.
17. Dabney J, Meyer M (2012) Length and GC-biases during sequencing library amplification: A comparison of various polymerase-buffer systems with ancient and modern DNA sequencing libraries. *Biotechniques* 52(2):87–94.
18. Meyer M, Kircher M (2010) Illumina sequencing library preparation for highly multiplexed target capture and sequencing. *Cold Spring Harb Protoc* 2010:pbp.prot5448.
19. Kircher M, Heyn P, Kelso J (2011) Addressing challenges in the production and analysis of illumina sequencing data. *BMC Genomics* 12:382.
20. Li H, Durbin R (2010) Fast and accurate long-read alignment with Burrows-Wheeler transform. *Bioinformatics* 26(5):589–595.
21. Krause J, et al. (2010) The complete mitochondrial DNA genome of an unknown hominin from southern Siberia. *Nature* 464(7290):894–897.
22. Li H, et al.; 1000 Genome Project Data Processing Subgroup (2009) The Sequence Alignment/Map format and SAMtools. *Bioinformatics* 25(16):2078–2079.
23. Posada D, Crandall KA (1998) MODELTEST: Testing the model of DNA substitution. *Bioinformatics* 14(9):817–818.
24. Wilgenbusch JC, Swofford D (2003) Inferring evolutionary trees with PAUP\*. *Curr Protoc Bioinformatics* Chapter 6:Unit 6.4.
25. Shapiro B, et al. (2011) A Bayesian phylogenetic method to estimate unknown sequence ages. *Mol Biol Evol* 28(2):879–887.
26. Drummond AJ, Suchard MA, Xie D, Rambaut A (2012) Bayesian phylogenetics with BEAUti and the BEAST 1.7. *Mol Biol Evol* 29(8):1969–1973.
27. Stiller M, et al. (2010) Withering away—25,000 years of genetic decline preceded cave bear extinction. *Mol Biol Evol* 27(5):975–978.
28. Keis M, et al. (2013) Complete mitochondrial genomes and a novel spatial genetic method reveal cryptic phylogeographical structure and migration patterns among brown bears in north-western Eurasia. *J Biogeogr* 40:915–927.
29. Kass RE, Raftery AE (1995) Bayes factors. *J Am Stat Assoc* 90:773–795.



**Table S1. Visual inspection and manual editing of alignment positions with consensus support <0.8**

Alignment position	Annotation	Coverage	Consensus support, %	Problem	Consensus call
1–138	D loop			Not targeted; repetitive region and flanking sequence	No consensus called
285	D loop	13	61.5	Alignment error around homopolymer stretch	Consensus corrected manually
757	D loop	51	78.4		
765	D loop	25	52	Three major sequence variants present in the region; one is identical to the reference and the other two match partial mitochondrial sequences of different bat species in a BLAST search	Consensus corrected manually after removing contaminant sequences
768	D loop	14	57.1		
1,815	16S rRNA	177	75.1		
1,820	16S rRNA	178	55.6		
1,822	16S rRNA	183	59		
1,823	16S rRNA	182	58.8		
1,837	16S rRNA	113	72.6		
2,006	16S rRNA	49	75.5	Two different sequence variants present; one variant is identical to the reference and the second matched bacterial sequences in a BLAST search	Consensus corrected manually after removing contaminant sequences
2,487	16S rRNA	4	75	One of four reads disagrees with reference; position is covered >60-fold and shows a single sequence variant supported by reads with terminal deamination patterns before subtraction of putative pig contaminants.	Consensus confirmed
3,416	NADH1	7	71.4	5C/2T; strand orientation compatible with cytosine deamination	Consensus confirmed
3,883	NADH1	3	66.7	2G/1A; strand orientation compatible with cytosine deamination	Consensus confirmed
5,398	tRNA-Trp	4	75	3C/1T; strand orientation compatible with cytosine deamination	Consensus confirmed
6,434	coxI	135	51.9	Region with excessive coverage and several sequence variants; one of the frequent variants matches bear by BLAST search and is supported by terminal deamination patterns in several sequences; all other variants match best to bacterial sequences	Consensus corrected manually after removing contaminant sequences
6,440	coxI	157	70.7		
6,443	coxI	156	61.5		
6,449	coxI	154	55.8		
6,455	coxI	145	78.6		
6,464	coxI	101	66.3		
6,609	coxI	9	77.8		
8,997–8999	atp6	1		Coverage too low	No consensus called
9,128	coxIII	9	55.6	5G/5A; one read with A shows four additional differences to the reference not shared by any other read (putative contaminant); strand orientation of the other 4 reads with A compatible with cytosine deamination	No consensus called
9,369	coxIII	3	66.7	2A/1G; strand orientation of only one read with A compatible with cytosine deamination	No consensus called
9,511	coxIII	3	66.7	Two reads with C, one with T; strand orientation of sequence with T compatible with cytosine deamination	Consensus confirmed
11,115	NADH4	8	75	6C/2T; strand orientation compatible with cytosine deamination	Consensus confirmed
11,189	NADH4	4	75	3C/1T; strand orientation compatible with cytosine deamination	Consensus confirmed
11,320	NADH4	4	75	3C/1T; strand orientation compatible with cytosine deamination	Consensus confirmed
13,613	NADH5	4	75	3C/1A; C additionally supported by a read with terminal C->T change	Consensus confirmed
13,803	NADH5	9	77.8	7G/2A; strand orientation compatible with cytosine deamination	Consensus confirmed
13,897	NADH5	4	75	One read with 3 substitutions and an insertion to the reference; BLAST search returns no significant similarity	Consensus confirmed after removing contaminant sequence
13,900	NADH5	4	75		
14,480	tRNA-Glu	3	66.7	2C/1T; strand orientation compatible with cytosine deamination	Consensus confirmed
15,343	cytb	7	71.4	5A/2G; reads with G show ≥ 2 t additional differences to reference and produce no hit to bear in BLAST search	Consensus confirmed after removing contaminant sequences

**Table S1. Cont.**

Alignment position	Annotation	Coverage	Consensus support, %	Problem	Consensus call
15,828–15,852	D loop	0–1		Coverage too low	No consensus called
15,920	D loop	9	66.7	Adjacent T and C homopolymer stretches; precise length of each stretch cannot be resolved	No consensus called for positions 15921–15937
15,923	D loop	14	64.3		
15,997–16,037	D loop	0–1		Coverage too low	No consensus called
16,112	D loop	44	70.5	Two different sequence variants present; one variants shows several mismatches to the reference and does not produce significant BLAST match	Consensus corrected manually after removing contaminant sequences
16,117	D loop	50	62		
16,132	D loop	72	58.3		
16,145	D loop	71	64.8		
16,430–16,783	D loop	0–1		Not targeted; repetitive region and flanking sequence	No consensus called

**Table S2. Cross-validation of molecular dates**

Sample	Radiocarbon age, YBP	Estimated mean age, YBP	95% HPD lower, YBP	95% HPD upper, YBP
SP232	27,230	27,951	24,091	33,757
SP234	<b>26,900</b>	<b>39,184</b>	<b>28,565</b>	<b>50,109</b>
SP891	44,160	33,689	24,091	45,243
SP1626	46,614	47,324	37,764	57,600
SP2027	27,180	26,729	24,090	31,097
SP2064	<b>44,050</b>	<b>80,194</b>	<b>49,200</b>	<b>118,257</b>
SP2106	24,210	27,873	24,090	34,272

YBP, years before present. Molecular estimates that are incongruent with radiocarbon dates are indicated in bold.

## Other Supporting Information Files

[Dataset S1 \(XLSX\)](#)